Research Article

Inactivation of GDP-fucose transporter gene (*Slc35c1*) in CHO cells by ZFNs, TALENs and CRISPR-Cas9 for production of fucose-free antibodies

Kah Fai Chan[1,2], Wahyu Shahreel[1], Corrine Wan[1], Gavin Teo[1], Noor Hayati[1], Shi Jie Tay[1], Wen Han Tong[1], Yuansheng Yang[1], Pauline M. Rudd[1], Peiqing Zhang[1,3], and Zhiwei Song[1,2]

[1]Bioprocessing Technology Institute, Agency for Science, Technology and Research (A*STAR), Centros, Singapore, Singapore

[2]Department of Biochemistry, Yong Loo Lin School of Medicine, National University of Singapore, Singapore

[3]Department of Anatomy, Yong Loo Lin School of Medicine, National University of Singapore, Singapore

Correspondence: Dr. Zhiwei Song, Bioprocessing Technology Institute, Agency for Science, Technology and Research (A*STAR), 20 Biopolis Way, #06-01 Centros, Singapore 138668, Singapore

E-mail: song_zhiwei@bti.a-star.edu.sg

Accepted Article

This article has been accepted for publication and undergone full peer review but has not been through the copyediting, typesetting, pagination and proofreading process, which may lead to differences between this version and the Version of Record. Please cite this article as doi: 10.1002/biot.201500331.

Submitted: 29-May-2015
Revised: 14-Aug-2015
Accepted: 07-Oct-2015

This article is protected by copyright. All rights reserved.

Keywords: CHO cells; Fucose-free antibodies; GDP-fucose transporter gene (SLC35C1); Genome editing technologies; Fluorescence-activated cell sorting (FACS)

Abbreviations: CHO, Chinese hamster ovary; C**HO-gmt**, CHO-glycosylation mutant; **EPO-Fc**, erythropoietin-Fc; **FBS**, fetal bovine serum; **ZFN**, zinc-figure nuclease; **TALEN**, transcription activator-like effector nuclease; **CRISPR-Cas9**, clustered regularly interspaced short palindromic repeat-CRISPR associated nuclease 9; **T7E1**, T7 endonuclease 1; **FACS**, fluorescence-activated cell sorting; **AAL**, *Aleuria aurantia* lectin; **MALDI-TOF MS**, matrix-assisted laser desorption/ionization time-of-flight mass spectrometry; **HILIC**, hydrophilic interaction chromatography; **UPLC**, ultra-performance liquid chromatography; **QTOF MS**, quadrupole time-of-flight mass spectrometry; **2-AB**, 2-aminobenzamide.

Accepted Article

Abstract

Removal of core fucose from *N*-glycans attached to human IgG1 significantly enhances its affinity for the receptor FcγRIII and thereby dramatically improves its antibody-dependent cellular cytotoxicity (ADCC) activity. While previous works have shown that inactivation of fucosyltransferase 8 (FUT8) results in mutants capable of producing fucose-free antibodies, we report here the use of genome editing techniques, namely ZFNs, TALENs and the CRISPR-Cas9, to inactivate the GDP-fucose transporter (SLC35C1) in CHO cells. A FACS approach coupled with a fucose-specific lectin was developed to rapidly isolate SLC35C1-deficient cells. Mass spectrometry analysis showed that both EPO-Fc produced in mutants arising from CHO-K1 and anti-Her2 antibody produced in mutants arising from a pre-existing antibody-producing CHO-HER line lacked core fucose. Lack of functional SLC35C1 in these cells does not affect cell growth or antibody productivity. Our data demonstrate that inactivating *Slc35c1* gene represents an alternative approach to generate CHO cells for production of fucose-free antibodies.

Accepted Article

1 Introduction

Recombinant human IgG1 antibodies used to target cancer cells are commonly produced in Chinese hamster ovary (CHO) cells. Both the Fab and Fc regions of the antibodies are required to carry out these activities. Binding of target antigen on cancer cells by the Fab region is followed by the engagement of the Fc region with the Fc receptor, FcγRIII, expressed on natural killer (NK) cells to kill the cancer cells via the antibody-dependent cellular cytotoxicity (ADCC) mechanism. Major sites of the Fc interaction with the FcγRIII are located in the hinge region and the CH2 domains of the antibody [1, 2]. In particular, this Fc-FcγRIII interaction is significantly affected by the glycan structures present at the conserved *N*-glycosylation site Asn^{297} in each of the CH2 domains [3]. It is now widely recognized that removal of the core fucose from the *N*-glycans of human IgG1 antibody significantly enhances its affinity towards FcγRIIIa, and therefore dramatically improves its ADCC activity [4, 5]. Enhanced *in vivo* ADCC by fucose-free antibodies has also been demonstrated in animal models and patients [6-9].

In mammalian cells, fucosylation reactions that take place in the Golgi apparatus frequently modify the *N*- and *O*-linked glycans, resulting in the formation of core fucose and the Lewis blood group antigens. Biochemical inhibitors for fucosylation reactions such as 2-fluorofucose and 5-alkynylfucose derivatives have been used to generate fucose-free antibodies [10]. Lec13 mutant CHO cells exhibit reduced activity of the GDP-mannose-4,6-dehydratase (GMD) and therefore reduced levels of GDP-fucose and fucosylated glycans [11]. In mammalian cells, GDP-fucose can be synthesized by two distinct pathways [12]. Loss-of-function mutations in the *GMD* gene can only affect the de novo pathway, not the salvage pathway. Therefore, Lec13 cells can produce IgG with reduced fucose content, not fucose-free antibodies.

Accepted Article

Although a total of 13 fucosyltransferases have been identified in mammalian genome, only α1,6 fucosyltransferase (FUT8) is able to transfer the core fucose to the *N*-glycans [12]. Consequently, FUT8 gene in CHO cells has been inactivated by homologous recombination [13] and zinc-finger nucleases (ZFNs) [14]. The substrate for fucosylation reactions, GDP-fucose, is synthesized in the cytosol and has to be transported into the Golgi or the endoplasmic reticulum (ER) by specific transporters in order to serve as the substrate for fucosylation reactions. The GDP-fucose transporter encoded by the *Slc35c1* gene transports GDP-fucose into the Golgi for core fucosylation. Meanwhile, a putative ER GDP-fucose transporter is believed to be encoded by *Slc35c2* gene [15]. Thus inactivation of *Slc35c1* gene can be an alternative strategy to prevent core fucosylation of *N*-glycans. It has been shown that loss-of-function mutation in the Golgi GDP-fucose transporter gene was able to eliminate all fucosylation reactions that occur in the Golgi [16, 17]. Therefore, we decided to inactivate the GDP-fucose transporter gene in CHO cells for production of fucose-free antibodies.

Three genome editing technologies developed recently have simplified the process of engineering cells for biologics production. Zinc-finger nucleases (ZFNs) are artificial restriction enzymes generated by fusion of zinc-finger DNA-binding domains normally found in transcription factors to the cleavage domain of restriction enzyme FokI [18-20]. The DNA-binding domain of ZFNs generally consists of three or four zinc-finger units. Each zinc-finger unit recognizes a 3-base pair (bp) stretch of DNA in the chromosome. Specificity of the ZFNs is determined by a motif of 7 amino acids within each zinc-finger. In order to allow the two FokI cleavage domains to dimerize and generate double-strand breaks (DSBs) in the chromosomal DNA, the two ZFNs must bind the opposite strands of the DNA and the two binding sites have to be separated by 5-7 bps. The DSBs created in the genomic DNA can then be repaired by error-prone non-homologous end joining (NHEJ) pathway which can create deletion or insertion mutations.

Accepted Article

Accepted Article

TALENs consist of customized transcription activator-like effector (TALE) fused to the catalytic domain of FokI nuclease [21, 22]. TALEs belong to a large family of transcription factors derived from plant pathogenic bacteria *Xanthomonas* spp. The DNA-binding domain of TALEs consists of several tandem repeats of 34 amino acids. Sequences of TALE repeats are highly conserved and differ mainly in two amino acid residues at positions 12 and 13, known as the repeat variable di-residues (RVDs). TALEs observe a simple cipher for DNA recognition where each repeat independently binds one nucleotide in the target DNA sequence as specified by the RVDs (where NI = A, HD = C, NG = T, NN = G or A) [23, 24]. Like ZFNs, TALENs function as a pair by binding to target DNA sequence on opposite DNA strands separated by a spacer of 12-21 bps and generate a DSB at the target site [22, 25].

The CRISPR (clustered regularly interspaced short palindromic repeats) -Cas9 (CRISPR-associated nuclease 9) system is a new technology for genome engineering. Unlike ZFNs and TALENs, Cas9 nuclease of the CRISPR-Cas9 system is recruited to the target site by a short guide RNA (gRNA). To inactivate a specific gene in mammalian cells, the cells are transfected by a vector that contains two transcription units. The expression of the short gRNA is controlled by a Pol III promoter such as U6 promoter and the synthesis of the Cas9 protein is controlled by a Pol II promoter such as CMV promoter. The gRNA associates itself with Cas9 protein and hybridizes with the target DNA in a sequence-specific manner by Watson-Crick base pairing. Each of the two active sites of Cas9 cleaves one strand of DNA to generate a DSB. In principle, any genomic region that matches the $GN_{20}GG$ sequence (where "N" can be any nucleotide) can be targeted by the CRISPR-Cas9 system [26-28].

In this paper, we report the inactivation of *Slc35c1* gene in CHO cells using ZFNs, TALENs and CRISPR-Cas9. Mutant cells generated by the different technologies were enriched and isolated by fluorescence-activated cell sorting (FACS) coupled with a fucose-specific *Aleuria aurantia* lectin (AAL). This approach dramatically improved the efficiency

of isolating mutant cells. A model glycoprotein, erythropoietin-Fc (EPO-Fc) fusion protein, produced by the mutant cells completely lacked the core fucose residues on their *N*-glycans. As ZFNs, TALENs and CRISPR-Cas9 technologies are all known to be able to generate off-target mutations which may affect cell growth and antibody productivity, the three technologies were also used to inactivate the same *Slc35c1* gene in a pre-existing anti-Her2 antibody-producing CHO cell line. The growth rates and anti-Her2 antibody productivities of mutant pools generated by the three technologies were compared.

Accepted Article

2 Materials and methods

2.1 Materials

Biotinylated AAL was purchased from Vector Laboratories (Burlingame, CA). Cy3-conjugated streptavidin was purchased from Jackson ImmunoResearch Laboratories Inc. (West Grove, PA). Trypsin was purchased from Promega Biosciences (San Luis Obispo, CA). PNGase F was purchased from Prozyme Inc. (San Leandro, CA). Hypercarb SPE cartridges and *N*-linked oligosaccharide standards were from Dextra Laboratories (Reading, UK). 2,5-Dihydroxybenzoic acid and Sep-Pak Vac C18 cartridge were from Waters Corporation (Milford, MA). Sodium acetate, ammonium carbonate, acetonitrile, methanol and sodium hydroxide were all of analytical grade from Merck KGaA (Darmstadt, Germany). Ultrapure water system from Sartorius (Goettingen, Germany) was utilized for analysis.

2.2 Cells and cell culture

CHO-K1 cells were obtained from the American Type Culture Collection (ATCC). CHO-K1 cells and CHO-gmt3 mutant cells were grown in Dulbecco's Modified Eagle's Medium (DMEM) from Life Technologies (Carlsbad, CA) supplemented with 10% FBS (Life Technologies), at 37°C with 5% CO_2. A trastuzumab (Herceptin)-producing CHO DG-44 cell line (CHO-HER) was generated as described previously [29]. CHO-HER and CHO-HER mutant pools with inactivated GDP-fucose transporter gene generated by ZFNs, TALENs and CRISPR-1 were cultured as 25 ml suspension culture in 125 ml shake flasks with chemically defined serum-free growth medium. The growth medium comprises HyClone™ PF-CHO™ (Thermo Scientific, Waltham, MA) and CD CHO (Life Technologies) at a 1:1 ratio, supplemented with 2 g/l sodium bicarbonate. The medium was also supplemented with 6

Accepted Article

mM glutamine (Life Technologies), and 0.05% Pluronic F-68 (Life Technologies). Cell density and viability were measured using the Trypan Blue exclusion method on an automated Vi-CELL XR Cell viability Analyzer from Beckman Coulter, Inc. (Brea, CA). Adherent cells were adapted to suspension cells via the in-house adaptation protocol through gradual reduction of serum into a serum-free protein-free medium.

2.3 Generation of ZFN constructs to target the Slc35c1 gene in CHO cells

The "modular assembly" method was used to generate the specific left and right zinc-finger nucleases (ZFNs) for targeting the Golgi GDP-fucose transporter (*Slc35c1)* gene in CHO cells. As described earlier [30], a DNA sequence in the first exon of the GDP-fucose transporter coding region, 5'-tAACCTCTGCCTCAAGTACGTAGGGGTGGCCt-3', was identified as the target site for ZFNs. The sequence of the seven amino acids in each zinc finger motif that determine the specificity of each finger was designed based on publically available information. The two ZFNs, ZFN-L and ZFN-R, used in this study were the same as those used in the previous report [30].

2.4 Generation of TALEN constructs to target the Slc35c1 gene in CHO cells

Transcription activator-like effector (TALE) repeat monomers (NI, NG, HD, NH) were synthesized as gBlocks (Integrated DNA Technologies (IDT) Inc., Coralville, IA) and cloned into pCR-Blunt II-TOPO® (Life Technologies) as templates for subsequent PCR reactions. The DNA sequences of these repeat monomers are derived from the 34 amino acid TALE repeat of *Xanthomonas sp*. AvrBs3 gene [31] and are codon-optimized for expression in CHO cells and also to reduce repetitiveness in assembled TALENs. Optimization of the sequence was carried out using the online IDT Codon Optimization tool

Accepted Article

(http://sg.idtdna.com/CodonOpt). Codon-optimized DNA fragments consisting of a nuclear localization signal in front of the truncated TALE N-terminal 136 amino acids (Δ152) of AvrBs3, and a 0.5 TALE repeat linked to +63 amino acid truncated C-terminal domain based on a previous report [22] were individually synthesized as gBlocks. These fragments were cloned sequentially into the multiple cloning site (MCS) of a modified pVax1 vector together with one of the two enhanced FokI domains to form the destination vector. Our destination vector uses a 25-bp sequence in place of the *ccdB* gene. FokI domains used are obligate heterodimers containing both Sharkey [32] and ELD:KKR [33] mutations for enhanced cleavage activity.

TALENs with 18.5 repeats were generated based on a modified Golden-Gate cloning methodology [34]. TALE repeats were PCR-amplified with position-specific primers to generate a library of monomers flanked by BsmBI and BsaI sites. The monomers were first assembled as hexamers into the array vector (a modified pcDNA3.1(+) vector containing BsmBI sites at the MCS and lacking BsaI sites) in a Golden Gate cloning reaction using BsmBI enzyme (Thermo Scientific) and T7 DNA ligase (New England Biolabs, Ipswich, MA). Hexamers were then assembled as an 18-mer into the destination vector between the TALE N-terminus and 0.5 repeat in a Golden-Gate cloning reaction using BsaI enzyme and T7 DNA ligase (New England Biolabs). This generates a fully assembled TALEN consisting of the TALE N-terminus, an 18.5-mer TALE repeat DNA binding domain and the TALE C-terminus linked to FokI domain.

To design a TALEN pair to target CHO cell *Slc35c1* gene, we analyzed the DNA sequence using the online tool TAL Effector Nucleotide Targeter 2.0 (https://talent.cac.cornell.edu/node/add/talen) [35, 36]. A potential target site in the first exon of the GDP-fucose transporter coding region was identified. It consists of two 20-bp TALE binding sites separated by a 19-bp spacer. The 34 amino acid TAL repeats used is of the form

Accepted Article

LTPEQVVAIASXXGGKQALETVQRLLPVLCQAHG where the underlined amino acids in the 12th and 13th position refer to the repeat variable di-residue (RVDs). The RVDs used for the TALENs are as follows: Left TALEN: NI HD HD NG NH HD NG NH NH NI HD NI NH HD HD HD HD NG HD; Right TALEN: NH NH NG NI NH NI NI NI NH NG NH NI HD NH NI NI NH NI NG.

2.5 Generation of CRISPR-Cas9 constructs to target the Slc35c1 gene in CHO cells

GeneArt® CRISPR Nuclease Vector kit was purchased from Life Technologies. Two CRISPR-Cas9 target sequences, both located in the first exon of the coding region in the CHO cell *Slc35c1* gene, were selected based on previous publications [26, 28]. To construct CRISPR-1 vector, the forward oligonucleotide was 5'-CGGGCGCTGCAGATCGCGCGTTTT -3', and the reverse oligonucleotide was 5'-GCGCGATCTGCAGCGCCCGCGGTG -3'. To construct CRISPR-2 vector, the forward oligonucleotide was 5'- TGCAAGGGCCTCAGCACTCGTTTT -3', and the reverse oligonucleotide was 5'- GAGTGCTGAGGCCCTTGCACGGTG -3'. Each pair of oligonucleotides was annealed and cloned into GeneArt® CRISPR Nuclease Vector by following manufacturer's instructions.

2.6 Transfection of CHO-K1 cells and anti-Her2 (trastuzumab) antibody-producing CHO DG44 cells (CHO-HER) with ZFNs, TALENs or CRISPR-Cas9 constructs

CHO-K1 cells were first seeded overnight at 6×10^5 cells per well of 6-well plates. Constructs expressing ZFNs or TALENs were transiently transfected into CHO-K1 cells using Lipofectamine LTX (Life Technologies) according to manufacturer's protocol. For

Accepted Article

each transfection, 2.5 μg of plasmid DNA (1.25 μg for each ZFN or TALEN) with 2.5 μl Plus reagent were mixed with 9 μl of Lipofectamine LTX reagent in 200 μl of Opti-MEM® I Reduced Serum Medium (OPTIMEM) (Life Technologies) and added to the cells in each well containing 2 ml of medium. Transfection medium was replaced with fresh culture medium at 8 hours post-transfection and cells were cultured for 3 days. Cells were then scaled up to T-75 flask and grown for another 3 days before undergoing AAL-staining and FACS.

Anti-Her2 (trastuzumab) antibody-producing CHO DG44 cells (CHO-HER) were transfected with ZFNs or TALENs targeting GDP-fucose transporter using 4D-Nucleofector™ (Lonza, Cologne, Germany) system according to manufacturer's protocol. Briefly, 1.5 million cells were harvested from exponentially growing suspension culture and washed with Dulbecco's phosphate buffered saline (DPBS) (Life Technologies). The cells were suspended in 100 μl of SG cell line Nucleofector™ solution containing 5 μg of plasmid DNA (2.5 μg for each ZFN or TALEN) in a Nucleocuvette™. Electroporation was then carried out using a Lonza 4D-Nucleofector™ X unit. Following transfection, cells were incubated in suspension in a 3 ml CD CHO : HyClone PF CHO medium in a 6-well plate overnight before they were transferred into a 25 ml fresh medium in a 125-ml shake flask for further culture. Cells were then harvested for AAL-staining and FACS at 7-10 days post-transfection.

For CRISPR-Cas9 modification, 5 million suspension CHO-K1 cells were electroporated using 4D-Nucleofector™ system with 5 μg of CRISPR-Cas9 plasmids in 100 μl of SG cell line Nucleofector™ solution. Following transfection, cells were recovered in growth medium in a suspension 6-well plate overnight before being scaled up to shake flask culture. Cells were then harvested for AAL-staining and FACS at 7-10 days post-transfection.

Accepted Article

Accepted Article

2.7 T7 endonuclease 1 (T7E1) mismatch assay

T7 endonuclease 1 (T7E1) was used to detect mutations mediated by ZFNs, TALENs and CRISPRs as described previously [37]. Genomic DNA of CHO cells transfected with ZFNs, TALENs or CRISPRs was extracted using DNeasy Blood & Tissue Kit (Qiagen, Hilden, Germany) at 72 hours post-transfection. PCR amplification of *Slc35c1* gene region encompassing the target sites was carried out for 35 cycles (95 °C, 30 s; 60 °C, 30 s; 68 °C, 40 s) using AccuPrime Taq DNA Polymerase High Fidelity Kit (Life Technologies) and the primer pair 5'-CCGTGGGGTGACCTAGCTCTT-3' and 5'-GCCACATGTGAGCAGGGCATAGAAG-3'. Purified PCR products were then heated and re-annealed slowly for heteroduplex formation. The reannealed DNA were then treated with 5 U of T7E1 (New England Biolabs) for 15 mins at 37°C and resolved on 2.5% TBE agarose gel. The gels were stained with RedSafe^{TM} staining solution (iNtRON Biotechnology, Gyeonggi, Korea) and analyzed on Gel Doc™ EZ imager using Image Lab™ Software (Bio-Rad). Gene modification activities were calculated using the formula % gene modification = $100 \times (1 - (1 - \text{fraction cleaved})^{1/2})$ as described previously [38].

2.8 Mutant cells in transfected CHO cells were enriched and isolated by FACS

To prepare for FACS, 1 x 10^7 transfected cells were harvested from a T-75 flask or 125-ml shake flask and washed twice with cold DPBS (Life Technologies). Blocking was carried out in 1% BSA/PBS (Sigma-Aldrich) for 30 min to prevent non-specific binding. Cells were then stained with 2 μg/ml biotinylated AAL (Vector Laboratories) in 1% BSA/PBS for 35 min. After two washes with cold DPBS, the stained cells were incubated with Cy3-conjugated streptavidin (Jackson ImmunoResearch Laboratories Inc.) at 2 μg/ml in 1% BSA/PBS for 35

min. After two more washes with cold DPBS, the cells were re-suspended in 2 ml of FACS buffer (DPBS containing 2% FBS) at a concentration of 5 x10^6 cells /ml prior to sorting. All incubation steps listed above were carried out on ice and sterile reagents were used. Cells were then subjected to FACSAria III cell sorter (Becton Dickinson Biosciences, Mountain View, CA). Single and viable cells were gated for by excluding debris and doublets on a series of forward scatter and side scatter dot plots (FSC-A vs. SSC-A, SSC-H vs. SSC-W, FSC-H vs. FSC-W). Cy3 signal was emitted using a blue laser (488 nm) excitation and fluorescence detected after passing through a bandpass filter 575/26 and 550 LP (Longpass) mirror. Sorted cells were collected and cultured in fresh medium supplemented with Antibiotic-Antimycotic (Life Technologies). Antibiotic-Antimycotic supplementation was then removed after 1 week of culture. For FACS of suspension CHO-K1 and CHO-HER cells, about 2-5 x 10^4 cells were collected into a single well of a 24-well plate containing 1 ml of growth medium containing serum and Antibiotics-Antimycotics. The sorted cells were allowed to recover in serum-containing medium for 4 days before they were scaled up into serum-free medium in 125-ml shake flask.

2.9 Molecular characterization of mutant clones

Genomic DNA from mutant clones was extracted using DNeasy Blood & Tissue Kit (Qiagen). PCR amplification of the targeted sites in the CHO cell *Slc35c1* gene was carried out for 28 cycles (95 °C, 30 s; 60 °C, 30 s; 68 °C, 45 s) using AccuPrime Pfx DNA Polymerase (Life Technologies) and the primer pair 5'-CCGTGGGGTGACCTAGCTCTT-3' and 5'-GCCACATGTGAGCAGGGCATAGAAG-3'. PCR products were gel-purified and cloned into pCR-Blunt II-TOPO® Vector (Life Technologies). 10 bacterial clones from each TOPO reaction were sequenced to characterize the mutation.

Accepted Article

Accepted Article

2.10 Genetic complementation of GDP-fucose transporter-deficient mutant clones

To check the phenotype of mutant clones, 4 x10^5 cells were seeded in 6-well plates overnight and transfected using Lipofectamine LTX (Life Technologies) with 2 μg of plasmid DNA encoding human GDP-fucose transporter (Accession number: NM_018389). For suspension-grown CHO-K1 and CHO-HER cells, 5 million cells were electroporated with 5 μg of plasmid DNA encoding human GDP-fucose transporter in SG cell line Nucleofector™ solution using 4D-Nucleofector™ system. 1-2 x10^6 cells were harvested two days after transfection. Cells were stained with biotinylated AAL and labeled with Cy3-streptavidin as described earlier and analyzed on the FACSAria cell sorter.

2.11 Transient expression of EPO-Fc in CHO-K1 and CHO-gmt3 for N-glycan analyses

Fc fusion protein of human erythropoietin (EPO-Fc) was produced in CHO-K1 and CHO-gmt3 cells as described earlier [39] for N-glycan structure analyses. Fc region from human IgG1 was fused to the C-terminus of EPO by overlap PCR. The PCR product for the EPO-Fc fusion was cloned into pcDNA3.1 with a Kozak sequence placed upstream of the translation start codon ATG. Cells were seeded overnight at 3 x 10^5 cells per ml into ten T-175 flasks. EPO-Fc construct was transiently transfected into CHO-K1 and CHO-gmt3 cells using Lipofectamine 2000 (Life technologies) with 60 μg of plasmid DNA per flask. At 6 hours post-transfection, cells were washed twice with PBS and replaced with chemically defined serum-free growth medium. Conditioned media containing secreted recombinant EPO-Fc were collected every 2 days over the course of 6 days, purified with a HiTrap Protein A HP column using an FPLC AKTA Purifier (GE Healthcare, Pittsburgh, PA). An amount of 200μg of purified EPO-Fc was used for carbohydrate structure analysis. The carbohydrates

liberated from the EPO-Fc by PNGase F were analyzed by MALDI-TOF mass spectrometry analysis as described previously [40].

2.12 Glycan release and purification

N-glycans were released directly from intact, purified glycoprotein samples, by PNGase F treatment. Briefly, glycoprotein samples, recombinant EPO-Fc, the in-house produced anti-Her2 antibody (trastuzumab) or Herceptin$^{\bigcirc,R}$ (produced by Roche), were first desalted using a PD 10 column (GE Healthcare, Pittsburgh, PA) following manufacturer's protocol. Then, an aliquot of the glycoprotein (20 μg for EPO-Fc or 100 μg for the anti-Her2 antibody) was mixed with 500 U of the PNGase F in the reaction buffer in a total volume of 100 μl and incubated at 37 ^{o}C for 1 h. Such conditions will result in complete deglycosylation of IgG and EPO-Fc as indicated by SDS-PAGE-capillary gel electrophoresis (data not shown). The released glycans were then purified by HyperCarb porous graphitized carbon cartridge (Thermo Fisher Scientific, CA), and dried by CentriVap (Labconco, Kansas City, MO) for subsequent analyses by matrix-assisted laser desorption/ionization time-of-flight mass spectrometry (MALDI-TOF MS) and hydrophilic interaction liquid chromatography - ultra performance liquid chromatography combined with quadrupole time-of-flight (HILIC-UPLC-QTOF).

2.13 Glycan profiling by MALDI-TOF MS

MALDI-TOF MS analysis of permethylated *N*-glycans was described in our previous report [29]. Briefly, the previously dried glycans were permethylated according to published protocols [41] and then cleaned up and fractioned into 15%, 35%, 50% and 75% (v/v) acetonitrile in water using a Sep-Pack C18 cartridge (Waters Corporation) [42]. Each elution

Accepted Article

fraction was dried under vacuum. Before MALDI-TOF MS acquisition, the dried permethylated glycan samples were dissolved in 30 µl of 80% (v/v) methanol in water. 0.5 µl of reconstituted sample was mixed with 0.5 µl of 2,5-dihydroxybenzoic acid (DHB) and then spotted onto the MALDI target plate. Mass spectra were acquired on a 5800 MALDI-TOF/TOF mass spectrometer (AB Sciex, Foster City, CA) in positive reflectron mode. Glycan structures were assigned to the respective peaks based on the matching mass-to-charge ratio (m/z) and knowledge of the *N*-glycan biosynthetic pathway in CHO cells.

2.14 Glycan analysis by HILIC-UPLC-QTOF

Quantitative analysis of *N*-glycan was performed by HILIC-UPLC-QTOF on a Waters UNIFI Biopharmaceutical platform (version 1.7, Waters Corporation). Briefly, the previously dried *N*-glycans were labelled with 2-aminobenzamide (2-AB) according to a published protocol [41]. The excess 2-AB was removed by passing the labeling mixture through a MiniTrap G-10 desalting column (GE Healthcare) and the purified 2-AB-labeled glycans were then dried under vacuum. Before analysis, the dried samples were reconstituted in 250 µl of solvent consisting of 70% (v/v) acetonitrile in water. 10 µl of the reconstituted 2-AB glycan sample was then injected to the UNIFI Biopharmaceutical platform. The entire platform consists of a UPLC-H class ultra-performance liquid chromatogram (UPLC) which is online-connected to a Xevo G2-S quadrupole-time of flight (QTOF) mass spectrometer, both under the control of UNIFI Biopharmaceutical software platform (version 1.7). The UPLC-H class consists of a sample manager (kept at 10 ^{o}C), a quaternary pump, a column oven (kept at 40 ^{o}C) which houses a Waters BEH Glycan column (2.1mm ID X 150 mm length), and a fluorescence detector. Glycans were separated on the HILIC column using a binary solvent system. Solvent A is 50 mM ammonium formate (pH 4.4) and solvent B is acetonitrile. The analytical run takes place in 16 min by ramping up the solvent A from 30%

Accepted Article

to 47%. The column was then flushed with 80% solvent A before re-equilibrated with 30% A for the next run. Glycan signal was detected at excitation wavelength of 330 nm and emission wavelength of 420 nm. Raw retention time of each chromatographic peak was converted to a glucose unit (GU) by fitting into a calibration curve established by a 2-AB-labeled dextran ladder (Waters Corporation). The GU value of each chromatographic peak was then used to search against an experimental database for *N*-glycans embedded in the UNIFI Biopharmaceutical platform. Primary assignment was done by alignment of observed and the expected GU values. In case of structural ambiguity, i.e. a GU value corresponding to more than one structure within the error tolerance (typically 0.1 GU), decision was then made based on accurate mass confirmation (5 ppm error) by the online ESI-QTOF and the possible biosynthetic pathway of *N*-glycans in CHO cells. The analytes were introduced into the QTOF under the following conditions: cone voltage: 80 kV; capillary voltage: 2.75 kV; source temperature: 120 ^{o}C; desolvation gas flow: 800 L/h; desolvation temperature: 300 ^{o}C. The QTOF was operated by scanning the mass range of 400 – 3,000 amu at the acquisition speed of 1 Hz. Mass accuracy was maintained by introducing a "lock spray" of Glu-fibrinopeptide (m/z = 785.8421).

2.15 Exoglycosidase digestions

The 2-AB-labeled glycans were digested with an array of exoglycosidases in 50 µl of 50 mM sodium acetate buffer (pH 5.5) for 18 h at 37°C according to a published protocol [43]. After the incubation, enzymes were removed by passing the mixture through a centrifugal filter cartridge with 10 (kDa) nominal molecular weight limit (NMWL) cut-off (Merck Millipore, Cork, Ireland). Digested, 2-AB-labeled glycans were collected in the flow-through and analyzed by the HILIC-UPLC-QTOF system.

Accepted Article

2.16 Growth and productivity analyses

CHO-gmt3 cells were first adapted to protein-free suspension shake flask culture. Viable cell density and cell viability of these mutant cell lines were examined. Cells were seeded at 2.5 x10^5 cells /ml in a 30 ml batch culture in triplicate samples and 1 ml fractions were collected at approximately 24-hour intervals for cell count. Cell density and viability from each sample were measured in duplicate using the Trypan blue exclusion method on an automated Vi-CELL XR Cell viability Analyzer (Beckman Coulter, Inc.). Growth and antibody titer (for CHO-HER cells) were analyzed until viability dropped below 50%. Antibody concentrations in 200 μl culture fractions were determined using the nephelometric method on an IMMAGE 800 immunochemistry system (Beckman Coulter, Inc.). Standard deviation (sd) was obtained from the cell count number for triplicate samples. Growth curve was plotted using mean ± sd.

Accepted Article

3 Results

3.1 Construction of ZFNs to target the *Slc35c1* gene in CHO cells

Based on published literature [18-20, 44-47], we designed a pair of ZFNs to target the *Slc35c1* gene in a CHO cell line [30]. A suitable target sequence was identified in the first exon of the coding region of the *Slc35c1* gene in CHO cells (Fig. 1A). In the current work, the two ZFNs for targeting the *Slc35c1* gene were the same as those used in the previous report [30].

3.2 Construction of TALENs to target the *Slc35c1* gene in CHO cells

To design a TALEN pair to target the *Slc35c1* gene in CHO cells, we analyzed the DNA sequence using the online tool TAL Effector Nucleotide Targeter 2.0 (https://talent.cac.cornell.edu/node/add/talen) [35, 36]. A suitable TALEN target site was identified in the first exon of the coding region (Fig. 1A). The 34-amino acid TAL repeats used are LTPEQVVAIASXXGGKQALETVQRLLPVLCQAHG where the RVDs (underlined) were NI, NG, HD and NH for binding A, T, C and G, respectively [23, 24, 48]. The DNA sequences of these repeat monomers were codon-optimized for expression in mammalian cells. Based on Miller's architecture [22], TALENs with 18.5 RVDs (having 20-bp specificity) were assembled by the Golden-Gate methodology with minor modifications as described in Materials and Methods [34]. The FokI domains contained both Sharkey [32] and ELD:KKR [33] mutations for enhanced cleavage activity.

Accepted Article

3.3 Construction of CRISPR-Cas9 expression constructs to target the *Slc35c1* gene in CHO cells

Several sites in the first exon of the coding region in the *Slc35c1* gene matched the $GN_{20}GG$ sequence and therefore can be selected as target sites for CRISPR-Cas9 [26, 28]. In this work, two CRISPR-Cas9 target sites were selected (Fig. 1A). For CRISPR-1, the target site is GCGGGCGCTGCAGATCGCGCTGG. For CRISPR-2, the target site is GTGCAAGGGCCTCAGCACTCTGG. One pair of oligonucleotides was synthesized for each CRISPR-Cas9 site. The oligonucleotides were annealed and cloned into GeneArt® CRISPR Nuclease Vector.

3.4 Mismatch assay to evaluate targeted DNA cleavage efficiency by the ZFNs, TALENs and CRISPRs

T7 endonuclease 1 (T7E1) was used to evaluate the cleavage activities mediated by the ZFNs, TALENs and CRISPRs as described previously [37]. Genomic DNA of CHO cells transfected with ZFNs, TALENs or CRISPRs was extracted 72 hours after transfection. The *Slc35c1* genomic region encompassing the target sites was amplified by PCR. Purified PCR products were then heated and reannealed slowly to permit the formation of heteroduplex between the mutated DNA strand and the wild-type DNA strand. The reannealed DNA samples were then treated with T7E1 and resolved on agarose gel (Fig. 1B). The expected sizes of the cleaved fragments are as indicated by the asterisk (*). The gene modification activities of TALEN, CRISPR-1 and CRISPR-2 were calculated to be 7.3%, 6.4% and 18.4%, according to the method by Guschin et al. [38]. The results suggest that CRISPR-2 has the highest gene modification activity. TALENs and CRISPR-1 are similarly efficient in generating mutations as the intensity levels of the cleaved DNA fragments are similar. ZFNs

Accepted Article

designed in this study appear to be the least efficient in generating mutations as suggested by the mismatch assay, as a result it was difficult to calculate the cleavage percentage.

3.5 The FACS approach to enrich and isolate GDP-fucose transporter deficient mutants generated by three different genome editing approaches

In our previous report [30], single clones were isolated two days after transfection with the plasmids encoding the ZFNs and screened by genomic PCR. Sequence analysis of the target locus was performed to identify mutations. This approach is both time consuming and labor intensive, and in many clones only one allele of the target gene is mutated. Therefore, we developed a lectin-based FACS method to enrich and isolate the mutants. The lectin, *Aleuria aurantia* lectin (AAL) that recognizes the core fucose on *N*-glycans [49] was used to identify mutant cells as the cells with fucose-free phenotype will not be stained by AAL.

To inactivate GDP-fucose transporter, wild-type CHO-K1 cells growing in a 6-well plate were first transfected with the plasmids encoding ZFNs, TALENs or CRISPRs. Two days after transfection, the cells were transferred into a T-75 flask and cultured to confluence. To prepare for FACS, 1 $x10^7$ transfected cells were incubated with biotinylated AAL and followed by Cy3-conjugated streptavidin. Stained cells were then sorted on a FACSAria cell sorter as shown in Fig. 2. FACS histogram of the first round of sorting revealed that most of the cells stained positive for AAL. The sorting gate for AAL-negative (AAL-ve) cells was set based on unstained CHO cells and this collected the lowest 0.5% of AAL-stained cells. About 1.2 $x10^4$ cells were collected from 3.5 $x10^6$ of each transfected cell pool. The collected AAL-ve cells were cultured for approximately 2 weeks and subjected to a second round of sorting. The AAL-ve cells collected from the second round of sorting were cultured and sorted again. For ZFNs-transfected cells, after first round of sorting AAL-ve cell population reached 50%

Accepted Article

of the total cells. For TALENs- and CRISPR-1-transfected cells, one round of sorting increased the AAL-ve cell population to more than 90% of the total cells (Fig. 2). These results (Fig. 2; Supporting information, Fig. S1) seem to correlate well with the differences in gene modification activities suggested by the T7E1 mismatch assay (Fig. 1B). Three rounds of sorting yielded a homogeneous population of AAL-ve cells from each transfected pool (Fig. 2). As a control, the same sorting procedure was repeated using untransfected CHO-K1 cells, no increase in AAL-ve population was observed (data not shown). To confirm that the cells with AAL-ve phenotype lacked functional GDP-fucose transporter, mutant pools were transfected with a plasmid encoding human GDP-fucose transporter. AAL analysis of the transfected cells revealed that the GDP-fucose transporter was able to rescue the AAL-ve phenotype generated by the ZFNs, TALENs and CRISPR-1 (Fig. 2).

Among the potential CRIPSR target sites that match the $GN_{20}GG$ sequence in the first exon of the coding region, two sites, CRISPR-1 and CRISPR-2, were selected in this work. As shown in Fig. 1B, CRISPR-2 showed highest gene modification activity. It is also more efficient in inactivating the *Slc35c1* gene as the first round of FACS showed a significant population of AAL-ve cells (14.6%) (Supporting information, Fig. S1). However, these cells failed to grow and eventually all died. This result could be attributed to the potential off-target effects. A BLAST search against the CHO cell genome suggests that CRISPR-1 shows less sequence matches at the 3' end (including the PAM sequence) compared to CRISPR-2 (red circles) (Supporting information, Fig. S2), suggesting that CRISPR-1 is likely to have less off-target effects and therefore is more specific [50, 51].

3.6 Molecular characterization of the CHO-gmt3 lines

CHO cells that lack functional GDP-fucose transporter due to mutated *Slc35c1* gene have been named CHO-gmt3 cells. To characterize the mutation in different CHO-gmt3 clones at

Accepted Article

the molecular level, single clones were isolated from the AAL-ve populations. All these single clones stained negatively with AAL and the AAL-ve phenotype was rescued by the human GDP-fucose transporter (data not shown). Genomic DNA from these clones was extracted and the *Slc35c1* locus was amplified by PCR. PCR products were then cloned into a TOPO vector and sequenced. The sequencing data revealed deletion or insertion mutations characteristic of NHEJ DNA repair at the respective ZFN, TALEN and CRISPR-1 cleavage sites (Table 1). Most clones showed two different mutations, suggesting that both alleles (A and B) of the *Slc35c1* gene have been mutated. In some CHO cell clones (ZFNs clones 5, 6 and 7; TALENs clones 4, 7 and 8; CRISPR-1 clone 7), only one type of mutation was observed after 10 bacteria TOPO clones were sequenced. One explanation is that there is only one allele of the *Slc35c1* gene in that particular cell. Another possibility could be loss of another mutant allele due to chromosomal translocation between DSBs at on-target site and off-target site [52]. Of course, it is also possible that both alleles happen to have the same mutation. Mutant clones with 3 mutated alleles were also detected (CRISPR-1 clone 8).

3.7 MALDI-TOF analysis of N-glycans released from recombinant EPO-Fc produced by CHO-gmt3 cells

For *N*-glycan analysis, EPO-Fc fusion protein was produced in wild-type CHO-K1 cells and one ZFN-inactivated CHO-gmt3 mutant clone (ZFNs clone 8 in Table 1). Recombinant EPO-Fc in the conditioned medium was purified by a Protein A column. The *N*-glycans attached to the purified EPO-Fc samples were then released by PNGase F and analyzed by MALDI-TOF MS as previously described [30, 39, 40]. Wild type CHO-K1 cells produced a mixture of mostly core-fucosylated complex *N*-glycans with bi-, tri-, and tetra-antennary structures sialylated with Neu5Ac residues (Supporting information, Fig. S3A). On the other hand, CHO-gmt3 produced fucose-free complex *N*-glycans with bi-, tri-, and tetra-

Accepted Article

antennary structures (Supporting information, Fig. S3B). These data confirmed that the loss of GDP-fucose transporter activity in CHO-gmt3 led to the production of glycoproteins with fucose-free *N*-glycans.

3.8 Inactivation of Slc35c1 gene in a pre-existing anti-Her2 antibody-producing CHO cell line

We next illustrate the direct application of the AAL-FACS approach to engineer an existing antibody-producing line to produce fucose-free antibodies. Suspension culture of a pre-existing CHO DG44 cell line, CHO-HER, that produces recombinant anti-Her2 antibody [29] was separately transfected with the same pair of ZFNs, TALENs and CRISPR-1 targeting the *Slc35c1* gene. 7-10 days post-transfection, the cells were subjected to the AAL-FACS procedure where the AAL-ve cells were collected and cultured (Supporting information, Fig. S4). Similarly, after 3 rounds of sorting, a homogeneous AAL-ve mutant population was obtained. Restoration of AAL positive (AAL+ve) phenotype upon transfection with the human GDP-fucose transporter cDNA confirms the successful inactivation of GDP-fucose transporter activity with three different technologies in the antibody-producing cell line.

3.9 Production of fucose-free anti-Her2 antibodies by the mutant cells

The parental CHO-HER and ZFN-inactivated GDP-fucose transporter mutant population CHO-HER (ZFNs) were grown in suspension batch culture in protein-free medium. The anti-Her2 antibody secreted into the medium was then harvested and purified. As a control, we have also included commercial Herceptin$^{\bigcirc,R}$ for the glycan analysis. *N*-glycans were released by PNGase F and analyzed by MALDI-TOF MS. Results showed that majority of the *N*-

Accepted Article

glycans released from Herceptin$^{\bigcirc,R}$ and parental CHO-HER-produced anti-Her2 are fucosylated with most abundant species being G0F, G1F and G2F (Fig. 3A & 3B). In contrast, the *N*-glycans produced by the mutant populations are fucose-free with majority of the structures being G0, G1 and G2 (Fig. 3C). As an orthogonal analysis, the released *N*-glycans were also examined by HILIC-UPLC-QTOF experiments. After labeling with 2-AB, the *N*-glycans were separated and profiled using HILIC-UPLC. Consistent glycan profiles of the samples were observed for both MALDI-TOF and HILIC-UPLC conditions. Similar to the MALDI-TOF MS data, HILIC-UPLC analysis of the *N*-glycans from Herceptin$^{\bigcirc,R}$ (Fig. 3D) and parental CHO-HER-produced anti-Her2 (Fig. 3E) revealed that the most abundant *N*-glycans are G0F, followed by G1F and G2F. The HILIC-UPLC profile of anti-Her2 produced by mutant CHO-HER (Fig. 3F) indicated the absence of fucosylated *N*-glycans. The amounts of each *N*-glycan presented as percentage of total *N*-glycans shown in Fig. 3D, 3E & 3F are summarized and compared. The results show that 91.54% of the *N*-glycans attached to Roche-produced Herceptin$^{\bigcirc,R}$ are fucosylated, 91.83% of the *N*-glycans released from the in-house-produced anti-Her2 antibody are fucosylated. The *N*-glycans produced by the mutant cells are completely lack of fucose (Supporting information, Table S1).

To resolve glycan structure ambiguity, glycans attached to the anti-Her2 antibody produced by the wild type parental CHO-HER cells (Fig. 4A) and the mutant CHO-HER cells (Fig. 4B) were further 'sequenced' through digestion with an array of exoglycosidases [53]. These results further confirmed the absence of fucosylation in anti-Her2 produced by mutant CHO-HER. Despite a slightly higher G1F % versus G0F % observed for anti-Her2 produced by parental CHO-HER (which can be attributed to culture conditions), we have shown that antibodies produced by mutant CHO-HER tend to have a similar *N*-glycan composition (fucose-free form) compared to Herceptin$^{\bigcirc,R}$. Collectively, these results support the feasibility of direct inactivation of GDP-fucose transporter with ZFNs, TALENs or

Accepted Article

CRISPR-Cas9 in antibody-producing CHO cells to generate mutant CHO cells that produce fucose-free antibodies.

3.10 Growth and productivity analysis of GDP-fucose transporter-deficient CHO-HER cells

To assess the suitability of the mutant cell lines generated by the ZFNs, TALENs or CRISPR for large-scale bioprocess and manufacturing of fucose-free antibodies, we tested the growth properties and productivity of these mutant lines. Adherent CHO-gmt3 mutant was adapted to protein-free suspension shake flask culture and we observed a growth pattern that was comparable to suspension wild-type CHO-K1 cells (data not shown). Growth pattern of CHO-HER and different mutant CHO-HER populations were also examined. Viable cell density and percentage viability of batch cultures of CHO-HER, CHO-HER (ZFNs), CHO-HER (TALENs) and CHO-HER (CRISPR-1) were measured over a course of 9 days and results were shown (Fig. 5A). CHO-HER (ZFNs), CHO-HER (TALENs) and CHO-HER (CRISPR-1) mutant pools exhibited comparable growth characteristics to their parental cell line CHO-HER with similar logarithmic, stationary and death phases.

In 2-L fed-batch bioreactor runs, the antibody productivity by the parental CHO-HER cells are constantly higher than 2 g/L (unpublished data). The amounts of antibodies produced in the media in the same set of shake flask batch cultures shown in Fig. 5A were determined at different time points from day 3 to day 9 (Fig. 5B). All three mutant populations shared a very similar growth profile to its parental CHO-HER cells (Fig. 5A), which demonstrates that inactivation of *Slc35c1* does not affect cells growth. The amounts of antibody produced by three mutant pools were compared with the parental CHO-HER cells (Fig. 5B). CHO-HER (TALENs) population showed similar antibody titer to the parental CHO-HER cells, suggesting that inactivation of the *Slc35c1* gene does not affect antibody

Accepted Article

productivity in CHO cells. The titers for CHO-HER (ZFNs) and CHO-HER (CRISPR-1) mutant pools, however, were lower compared to the parental line.

To address this issue, we randomly picked 6 single clones from the CHO-HER (CRISPR-1) mutant pool and a similar shake flask batch culture experiment was carried out. The growth profiles of the parental CHO-HER cells and the 6 CHO-HER (CRISPR-1) clones were similar (Fig. 5C). However, only Clone 1 exhibited a similar productivity as the parental CHO-HER cells, whereas others showed reduced productivities (Fig. 5D). Whether the reduced productivities observed in these pools is due to off-target effects remains to be investigated. Nonetheless, high producing clones can be isolated from the mutant pools generated by the CRISPR-Cas9 technology. The same may be true for the ZFNs-generated pool.

Accepted Article

4 Discussion

In mammalian cells, two pathways lead to the production of GDP-fucose, namely the *de novo* pathway and the salvage pathway. CHO Lec13 cells have a mutation in the GDP-mannose dehydratase gene in the *de novo* pathway that reduces the amount of GDP-fucose in the cell but does not completely eliminate core fucosylation [11]. A total of thirteen fucosyltransferases have been characterized, only FUT8 possesses α1,6-transferase activity with the ability to transfer fucose to the core position on *N*-glycans [12]. Inactivation of *Fut8* gene has been shown to prevent core fucosylation in CHO cells [35]. It is known that in wild-type CHO cells, core fucose is the only fucose present on the *N*-glycans [42]. The exceptions are CHO cell mutants LEC11 and LEC12 that carry novel gain-of-function mutations and express sialyl Lewis^X epitope [54]. No fucose is found on the shortened mucin type *O*-glycans [42]. The CHO-K1 transcriptome data have shown that among all fucosyltransferases, only FUT8 and two protein O-fucosyltransferases (POFUT-1 and POFUT-2) are expressed [55]. As both POFUT-1 and POFUT-2 are localized in the ER [56,57], protein O-fucosylation by POFUT-1 and POFUT-2 will not be affected as SLC35C1 is only responsible for transporting GDP-fucose into the Golgi. Therefore, the only fucosyltransferase that should be affected by inactivating the Golgi GDP-fucose transporter gene (*Slc35c1*) is FUT8. As such, inactivating *Fut8* or *Slc35c1* should have similar impact on CHO-K1 cells. A potential advantage of knocking out *Slc35c1* over *Fut8* is that it eliminates the potential complications caused by the gain-of-function mutations found in LEC11 and LEC12 cells [54]. Our results have shown that inactivation of *Slc35c1* gene in CHO cells did not seem to affect cell growth, viable cell density and antibody productivity. Data presented in this report suggest that inactivation of GDP-fucose transporter in CHO cells represents a feasible strategy for production of fucose-free antibodies.

Accepted Article

Accepted Article

Three different genome-editing technologies were used to inactivate GDP-fucose transporter in CHO cells. For ZFNs, based on data from published literature, we have assembled a pair of ZFNs to target GDP-fucose transporter. Essentially, the array of zinc-finger units can be re-assembled using different finger units to target different DNA sequences by the modular assembly method [58]. However, the ZFNs design is often complicated by context dependent effects of zinc-finger units arising from crosstalk between zinc-fingers and overlap effects of 3-bp target sites. Engineering and screening for a ZFN pair with high binding affinity and specificity to target a given DNA sequence require special expertise and resources.

TALENs represent a more modular mode of DNA recognition. The one-to-one correspondence between the RVDs and target nucleotides means that site-specific TALEs can be designed by having the linear array of TALE repeats matching to target DNA sequence in the 5' to 3' direction. Various methods to assemble TALENs have been reported [34, 35, 59, 60] and we found the Golden-Gate methodology to be a relatively easy method. The main disadvantage with TALENs is that it is still not clearly understood why certain assembled TALENs work and others do not.

The major advantage of the CRISPR-Cas9 system lies in the easy design of gRNAs and high gene modification efficiency. Unlike ZFNs and TALENs that rely on protein-DNA interactions to recognize target sites in the chromosome, CRISPR-Cas9 system recognizes target sites by Watson-Crick base pairing between gRNA and DNA sequence. Multiple gRNAs can be introduced simultaneously to enable editing of multiple genes in the same cell [26, 28]. A major caveat with the use of CRISPR system is that it tolerates base pair mismatches between gRNA and its complementary target sequence primarily at the 5' end >12-bp from the PAM sequence [26] and up to 6-bp mismatches at the target site [27]. However, this can be circumvented by the use of nickases in the form of mutant Cas9 to

generate targeted mutagenesis in the presence of donor template by HDR to reduce off-target effects [26, 27].

Although the CRISPR-Cas9 technology is easy to use for cell line engineering, potential off-target effect remains to be a potential problem. As we have shown in this study, antibody productivity of the mutant pool generated by TALENs is comparable to that of the parental cells, whereas the productivity of the mutant pools generated by ZFNs and CRISPR-1 decreased, despite all having similar growth profiles to the parental CHO-HER cell line. Whether the reduced antibody productivity in CHO-HER (ZFNs) and CHO-HER (CRISPR-1) mutant pools was due to off-target effect are being investigated.

The use of FACS approach allows us to enrich for genetically-engineered mutants with the desired phenotype. This is in contrast to previous strategies of identifying genotype which can be time-consuming. Importantly, fucose-free antibody-producing cell lines can be rapidly generated from pre-existing antibody-producing lines in less than two months. We have also demonstrated that the FACS approach is effective in isolating mutants engineered by custom nucleases having low gene modification activity. Apart from lectins, we believe that antibodies specific for certain cell surface antigens can also be used in this FACS approach to select for ZFN/TALEN/CRISPR-engineered cells.

Accepted Article

Acknowledgement:

This work was supported in part by the Strategic Positioning Fund (SPF2013/001) ("GlycoSing") from the Biomedical Research Council (BMRC) of Agency for Science, Technology and Research (A*STAR), Singapore and A*STAR's Joint Council (JCO) Visiting Investigator Programme ("HighGlycoART"). The authors thank Ms. Jessna Yeo for her technical assistance and Dr. Natasha Ann Pereira and Mr. Ryan Haryadi for reviewing the manuscript.

The authors declare no financial or commercial conflict of interest.

Accepted Article

Accepted Article

5 References

[1] Radaev, S., Motyka, S., Fridman, W. H., Sautes-Fridman, C., Sun, P. D., The structure of a human type III Fcgamma receptor in complex with Fc. *J. Biol. Chem.* 2001, *276*, 16469-16477.

[2] Sondermann, P., Huber, R., Oosthuizen, V., Jacob, U., The 3.2-A crystal structure of the human IgG1 Fc fragment-Fc gammaRIII complex. *Nature* 2000, *406*, 267-273.

[3] Krapp, S., Mimura, Y., Jefferis, R., Huber, R., Sondermann, P., Structural analysis of human IgG-Fc glycoforms reveals a correlation between glycosylation and structural integrity. *J. Mol. Biol.* 2003, *325*, 979-989.

[4] Shields, R. L., Lai, J., Keck, R., O'Connell, L. Y.*, et al.*, Lack of fucose on human IgG1 N-linked oligosaccharide improves binding to human Fcgamma RIII and antibody-dependent cellular toxicity. *J. Biol. Chem.* 2002, *277*, 26733-26740.

[5] Shinkawa, T., Nakamura, K., Yamane, N., Shoji-Hosaka, E.*, et al.*, The absence of fucose but not the presence of galactose or bisecting N-acetylglucosamine of human IgG1 complex-type oligosaccharides shows the critical role of enhancing antibody-dependent cellular cytotoxicity. *J. Biol. Chem.* 2003, *278*, 3466-3473.

[6] Cardarelli, P. M., Moldovan-Loomis, M. C., Preston, B., Black, A.*, et al.*, In vitro and in vivo characterization of MDX-1401 for therapy of malignant lymphoma. *Clin. Cancer Res.* 2009, *15*, 3376-3383.

[7] Junttila, T. T., Parsons, K., Olsson, C., Lu, Y.*, et al.*, Superior in vivo efficacy of afucosylated trastuzumab in the treatment of HER2-amplified breast cancer. *Cancer Res.* 2010, *70*, 4481-4489.

[8] Niwa, R., Hatanaka, S., Shoji-Hosaka, E., Sakurada, M.*, et al.*, Enhancement of the antibody-dependent cellular cytotoxicity of low-fucose IgG1 Is independent of FcgammaRIIIa functional polymorphism. *Clin. Cancer Res.* 2004, *10*, 6248-6255.

[9] Suzuki, E., Niwa, R., Saji, S., Muta, M.*, et al.*, A nonfucosylated anti-HER2 antibody augments antibody-dependent cellular cytotoxicity in breast cancer patients. *Clin. Cancer Res.* 2007, *13*, 1875-1882.

[10] Okeley, N. M., Alley, S. C., Anderson, M. E., Boursalian, T. E.*, et al.*, Development of orally active inhibitors of protein and cellular fucosylation. *Proc Natl Acad Sci U S A.* 2013, *110*, 5404-5409.

[11] Ohyama, C., Smith, P. L., Angata, K., Fukuda, M. N.*, et al.*, Molecular cloning and expression of GDP-D-mannose-4,6-dehydratase, a key enzyme for fucose metabolism defective in Lec13 cells. *J. Biol. Chem.* 1998, *273*, 14582-14587.

[12] Becker, D. J., Lowe, J. B., Fucose: biosynthesis and biological function in mammals. *Glycobiology* 2003, *13*, 41R-53R.

[13] Yamane-Ohnuki, N., Kinoshita, S., Inoue-Urakubo, M., Kusunoki, M.*, et al.*, Establishment of FUT8 knockout Chinese hamster ovary cells: an ideal host cell line for producing completely defucosylated antibodies with enhanced antibody-dependent cellular cytotoxicity. *Biotechnol. Bioeng.* 2004, *87*, 614-622.

[14] Malphettes, L., Freyvert, Y., Chang, J., Liu, P. Q.*, et al.*, Highly efficient deletion of FUT8 in CHO cell lines using zinc-finger nucleases yields cells that produce completely nonfucosylated antibodies. *Biotechnol. Bioeng.* 2010, *106*, 774-783.

[15] Lu, L., Hou, X., Shi, S., Korner, C., Stanley, P., Slc35c2 promotes Notch1 fucosylation and is required for optimal Notch signaling in mammalian cells. *J. Biol. Chem.* 2010, *285*, 36245-36254.

[16] Lubke, T., Marquardt, T., Etzioni, A., Hartmann, E.*, et al.*, Complementation cloning identifies CDG-IIc, a new type of congenital disorders of glycosylation, as a GDP-fucose transporter deficiency. *Nat. Genet.* 2001, *28*, 73-76.

Accepted Article

[17] Luhn, K., Wild, M. K., Eckhardt, M., Gerardy-Schahn, R., Vestweber, D., The gene defective in leukocyte adhesion deficiency II encodes a putative GDP-fucose transporter. *Nat. Genet.* 2001, *28*, 69-72.
[18] Doyon, Y., McCammon, J. M., Miller, J. C., Faraji, F.*, et al.*, Heritable targeted gene disruption in zebrafish using designed zinc-finger nucleases. *Nat. Biotechnol.* 2008, *26*, 702-708.
[19] Miller, J. C., Holmes, M. C., Wang, J., Guschin, D. Y.*, et al.*, An improved zinc-finger nuclease architecture for highly specific genome editing. *Nat. Biotechnol.* 2007, *25*, 778-785.
[20] Urnov, F. D., Miller, J. C., Lee, Y. L., Beausejour, C. M.*, et al.*, Highly efficient endogenous human gene correction using designed zinc-finger nucleases. *Nature* 2005, *435*, 646-651.
[21] Christian, M., Cermak, T., Doyle, E. L., Schmidt, C.*, et al.*, Targeting DNA double-strand breaks with TAL effector nucleases. *Genetics* 2010, *186*, 757-761.
[22] Miller, J. C., Tan, S., Qiao, G., Barlow, K. A.*, et al.*, A TALE nuclease architecture for efficient genome editing. *Nat. Biotechnol.* 2011, *29*, 143-148.
[23] Boch, J., Scholze, H., Schornack, S., Landgraf, A.*, et al.*, Breaking the code of DNA binding specificity of TAL-type III effectors. *Science* 2009, *326*, 1509-1512.
[24] Moscou, M. J., Bogdanove, A. J., A simple cipher governs DNA recognition by TAL effectors. *Science* 2009, *326*, 1501.
[25] Kim, Y., Kweon, J., Kim, A., Chon, J. K.*, et al.*, A library of TAL effector nucleases spanning the human genome. *Nat. Biotechnol.* 2013, *31*, 251-258.
[26] Cong, L., Ran, F. A., Cox, D., Lin, S.*, et al.*, Multiplex genome engineering using CRISPR/Cas systems. *Science* 2013, *339*, 819-823.
[27] Jinek, M., Chylinski, K., Fonfara, I., Hauer, M.*, et al.*, A programmable dual-RNA-guided DNA endonuclease in adaptive bacterial immunity. *Science* 2012, *337*, 816-821.
[28] Mali, P., Yang, L., Esvelt, K. M., Aach, J.*, et al.*, RNA-guided human genome engineering via Cas9. *Science* 2013, *339*, 823-826.
[29] Ho, S. C., Bardor, M., Feng, H., Mariati*, et al.*, IRES-mediated Tricistronic vectors for enhancing generation of high monoclonal antibody expressing CHO cell lines. *J Biotechnol* 2012, *157*, 130-139.
[30] Zhang, P., Haryadi, R., Chan, K. F., Teo, G.*, et al.*, Identification of functional elements of the GDP-fucose transporter SLC35C1 using a novel Chinese hamster ovary mutant. *Glycobiology* 2012, *22*, 897-911.
[31] Bonas, U., Stall, R. E., Staskawicz, B., Genetic and structural characterization of the avirulence gene avrBs3 from Xanthomonas campestris pv. vesicatoria. *Mol. Gen. Genet.* 1989, *218*, 127-136.
[32] Guo, J., Gaj, T., Barbas, C. F., 3rd, Directed evolution of an enhanced and highly efficient FokI cleavage domain for zinc finger nucleases. *J. Mol. Biol.* 2010, *400*, 96-107.
[33] Doyon, Y., Vo, T. D., Mendel, M. C., Greenberg, S. G.*, et al.*, Enhancing zinc-finger-nuclease activity with improved obligate heterodimeric architectures. *Nat. Methods* 2011, *8*, 74-79.
[34] Sanjana, N. E., Cong, L., Zhou, Y., Cunniff, M. M.*, et al.*, A transcription activator-like effector toolbox for genome engineering. *Nat Protoc* 2012, *7*, 171-192.
[35] Cermak, T., Doyle, E. L., Christian, M., Wang, L.*, et al.*, Efficient design and assembly of custom TALEN and other TAL effector-based constructs for DNA targeting. *Nucleic Acids Res.* 2011, *39*, e82.
[36] Doyle, E. L., Booher, N. J., Standage, D. S., Voytas, D. F.*, et al.*, TAL Effector-Nucleotide Targeter (TALE-NT) 2.0: tools for TAL effector design and target prediction. *Nucleic Acids Res.* 2012, *40*, W117-122.

[37] Kim, H. J., Lee, H. J., Kim, H., Cho, S. W., Kim, J. S., Targeted genome editing in human cells with zinc finger nucleases constructed via modular assembly. *Genome Res.* 2009, *19*, 1279-1288.
[38] Guschin, D. Y., Waite, A. J., Katibah, G. E., Miller, J. C*., et al.*, A rapid and general assay for monitoring endogenous gene modification. *Methods Mol Biol.* 2010, *649*, 247-256.
[39] Goh, J. S., Zhang, P., Chan, K. F., Lee, M. M*., et al.*, RCA-I-resistant CHO mutant cells have dysfunctional GnT I and expression of normal GnT I in these mutants enhances sialylation of recombinant erythropoietin. *Metab Eng.* 2010, *12*, 360-368.
[40] Lim, S. F., Lee, M. M., Zhang, P., Song, Z., The Golgi CMP-sialic acid transporter: A new CHO mutant provides functional insights. *Glycobiology* 2008, *18*, 851-860.
[41] Dell, A., Reason, A. J., Khoo, K. H., Panico, M*., et al.*, Mass spectrometry of carbohydrate-containing biopolymers. *Methods Enzymol.* 1994, *230*, 108-132.
[42] North, S. J., Huang, H. H., Sundaram, S., Jang-Lee, J*., et al.*, Glycomics profiling of Chinese hamster ovary cell glycosylation mutants reveals N-glycans of a novel size and complexity. *J. Biol. Chem.* 2010, *285*, 5759-5775.
[43] Shahrokh, Z., Royle, L., Saldova, R., Bones, J*., et al.*, Erythropoietin produced in a human cell line (Dynepo) has significant differences in glycosylation compared with erythropoietins produced in CHO cell lines. *Mol. Pharm.* 2011, *8*, 286-296.
[44] Dreier, B., Segal, D. J., Barbas, C. F., 3rd, Insights into the molecular recognition of the 5'-GNN-3' family of DNA sequences by zinc finger domains. *J. Mol. Biol.* 2000, *303*, 489-502.
[45] Liu, Q., Xia, Z., Zhong, X., Case, C. C., Validated zinc finger protein designs for all 16 GNN DNA triplet targets. *J. Biol. Chem.* 2002, *277*, 3850-3856.
[46] Segal, D. J., Dreier, B., Beerli, R. R., Barbas, C. F., 3rd, Toward controlling gene expression at will: selection and design of zinc finger domains recognizing each of the 5'-GNN-3' DNA target sequences. *Proc Natl Acad Sci U S A.* 1999, *96*, 2758-2763.
[47] Sander, J. D., Zaback, P., Joung, J. K., Voytas, D. F., Dobbs, D., Zinc Finger Targeter (ZiFiT): an engineered zinc finger/target site design tool. *Nucleic Acids Res.* 2007, *35*, W599-605.
[48] Cong, L., Zhou, R., Kuo, Y. C., Cunniff, M., Zhang, F., Comprehensive interrogation of natural TALE DNA-binding modules and transcriptional repressor domains. *Nat. Commun.* 2012, *3*, 968.
[49] Matsumura, K., Higashida, K., Ishida, H., Hata, Y*., et al.*, Carbohydrate binding specificity of a fucose-specific lectin from Aspergillus oryzae: a novel probe for core fucose. *J. Biol. Chem.* 2007, *282*, 15700-15708.
[50] Kuscu, C., Arslan, S., Singh, R., Thorpe, J., Adli, M., Genome-wide analysis reveals characteristics of off-target sites bound by the Cas9 endonuclease. *Nat. Biotechnol.* 2014, *32*, 677-683.
[51] Wu, X., Scott, D. A., Kriz, A. J., Chiu, A. C*., et al.*, Genome-wide binding of the CRISPR endonuclease Cas9 in mammalian cells. *Nat. Biotechnol.* 2014, *32*, 670-676.
[52] Frock, R. L., Hu, J., Meyers, R. M., Ho, Y. J., et al., Genome-wide detection of DNA double-stranded breaks induced by engineered nucleases. *Nat. Biotechnol.* 2015, 33, 179-186.
[53] Marino, K., Bones, J., Kattla, J. J., Rudd, P. M., A systematic approach to protein glycosylation analysis: a path through the maze. *Nat. Chem. Biol.* 2010, *6*, 713-723.
[54] Howard, D. R., Fukuda, M., Fukuda, M. N., Stanley, P., The GDP-fucose:N-acetylglucosaminide 3-alpha-L-fucosyltransferases of LEC11 and LEC12 Chinese hamster ovary mutants exhibit novel specificities for glycolipid substrates. *J. Biol. Chem.* 1987, *262*, 16830-16837.

Accepted Article

[55] Xu, X., Nagarajan, H., Lewis, N. E., Pan, S.*, et al.*, The genomic sequence of the Chinese hamster ovary (CHO)-K1 cell line. *Nat. Biotechnol.* 2011, *29*, 735-741.
[56] Luo, Y., Haltiwanger, R. S., O-fucosylation of notch occurs in the endoplasmic reticulum. *J. Biol. Chem.* 2005, *280*, 11289-11294.
[57] Luo, Y., Koles, K., Vorndam, W., Haltiwanger, R. S., Panin, V. M., Protein O-fucosyltransferase 2 adds O-fucose to thrombospondin type 1 repeats. *J. Biol. Chem.* 2006, *281*, 9393-9399.
[58] Bhakta, M. S., Segal, D. J., The generation of zinc finger proteins by modular assembly. *Methods Mol. Biol.* 2010, *649*, 3-30.
[59] Reyon, D., Tsai, S. Q., Khayter, C., Foden, J. A.*, et al.*, FLASH assembly of TALENs for high-throughput genome editing. *Nat. Biotechnol.* 2012, *30*, 460-465.
[60] Schmid-Burgk, J. L., Schmidt, T., Kaiser, V., Honing, K., Hornung, V., A ligation-independent cloning technique for high-throughput assembly of transcription activator-like effector genes. *Nat. Biotechnol.* 2013, *31*, 76-81.

Accepted Article

Table 1. **Mutations in the GDP-fucose transporter gene in CHO cells generated by the ZFNs, TALENs and CRISPR-1.** Wild type (WT) sequence for each target site is shown on top. Binding sequences by the ZFNs, TALENs or CRISPR-1 are highlighted in red. Clone names are shown on the left. Deletion mutations (--) or insertion mutations (bases highlighted in blue) are summarized on the right. *: partial DNA substitution.

Mutations introduced by the ZFNs:

```
WT  ATGATAAGTTTCAATAACCTCTGCCTCAAGTACGTAGGGGTGGCCTTCTACAACGTGGGGCGCTCG
1A  ATGATAAGTTTCAATAACCTCTGCCTCAAG--CGTAGGGGTGGCCTTCTACAACGTGGGGCGCTCG          -2
1B  ATGATAAGTTTCAATAACCT----------------------------------TGGGGCGCTCG          -35
2A  ATGATAAGTTTCAATAACCTCTGCCTCAAG--CGTAGGGGTGGCCTTCTACAACGTGGGGCGCTCG          -2
2B  ATGATAAGTTTCAATAACCT----------------------------------TGGGGCGCTCG          -35
3A  ATGATAAGTTTCAATAACCTCTGCCTCAAGTA--TAGGGGTGGCCTTCTACAACGTGGGGCGCTCG          -2
3B  ATGATAAGTTTCAATAACCTCTGCCTCAAGTAGTACGTAGGGGTGGCCTTCTACAACGTGGGGCGC          +3
4A  ATGATAAGTTTCAATAACCTCTGCCTCAAG--CGTAGGGGTGGCCTTCTACAACGTGGGGCGCTCG          -2
4B  ATGATAAGTTTCAATAACCTCTGCCTCAAAGTACGTAGGGGTGGCCTTCTACAACGTGGGGCGCTC          +1
5   ATGATAAGTTTCAATAACCTCTGCCTCAAGTA--TAGGGGTGGCCTTCTACAACGTGGGGCGCTCG          -2
6   ATGATAAGTTTCAATAACCTCTG--------------------GCCTTCTACAACGTGGGGCGCTCG          -19
7   ATGATAAGTTTCAATAACCTCTGCCTCA--------GGGGTGGCCTTCTACAACGTGGGGCGCTCG          -8
8A  ATGATAAGTTTCAATAACCTCTGCCTCAAG--CGTAGGGGTGGCCTTCTACAACGTGGGGCGCTCG          -2
8B  ATGATAAGTTTCAATAACCT----------------------------------TGGGGCGCTCG          -35
9A  ATGATAAGTTTCAATAACCTCTGCCTCAAGTA--TAGGGGTGGCCTTCTACAACGTGGGGCGCTCG          -2
9B  ATGATAAGTTTCAATAACCTCTGCCTCAAGTAGGATGTGCTTGGTCCGGGAAGACCTGTCACTGAA          +108
    GTTACGCATGCAGATTCGACACTGGAAGGGCCTCTCAGCTGTCGTGCCAGCTGCATTAATGAATCG
    GCCAAGTACGTAGGGGTGGCCTTCTACAACGTGGGGCGCTCG
```

Mutations introduced by the TALENs:

```
WT  CTCAACAAGTACCTGCTGGACAGCCCCTCCCTGCAGCTGGATACCCCTATCTTCGTCACTTTCTACCAATGCCT
1A  CTCAACAAGTACCTGCTGGACAGCCCCTCCCTGCAGC-GGATACCCCTATCTTCGTCACTTTCTACCAATGCCT  -1
1B  CTCAACAAGTACCTGCTGGACAGCCCCTCCCT----------------ATCTTCGTCACTTTCTACCAATGCCT  -16
2A  CTCAACAAGTACCTGCTGGACAGCCCCTCCCTGCAGCTTGGATACCCCTATCTTCGTCACTTTCTACCAATGCC  +1
2B  C-------------------------------------------CTATCTTCGTCACTTTCTACCAATGCCT  -45
3A  CTCAACAAGTACCTGCTGGACAGCCCCTCCCTGCAGCTGGGGATACCCCTATCTTCGTCACTTTCTACCAATGC  +2
3B  CTCAACAAGTACCTGCTGGACAGCCCCTCCCTGCTGTCACTTTCTACCTATCTTCGTCACTTTCTACCAATGCC  +1*
4   CTCAACAAGTACCTGCTGGACAGCCCCTCCCTGCAGCTTGGATACCCCTATCTTCGTCACTTTCTACCAATGCC  +1
5A  CTCAACAAGTACCTGCTGGACAGCCCCTCCCTGCAGCTGTTGGTACCCCTATCTTCGTCACTTTCTACCAATGC  +2*
5B  CTCAACAAGTACCTGCTGGACAGCCCCTCCCTGCAGC-----ACCCCTATCTTCGTCACTTTCTACCAATGCCT  -5
6A  CTCAACAAGTACCTGCTGGACAGCCCCTCCCTGCAGCTTGGATACCCCTATCTTCGTCACTTTCTACCAATGCC  +1
6B  CTCAACAAGTACCTGCTGGAC----------------------CCTATCTTCGTCACTTTCTACCAATGCCT  -24
7   CTCAACAAGTACCTGCTGGACAGCCCCTCCCTGCAGCA--ATACCCCTATCTTCGTCACTTTCTACCAATGCCT  -2*
8   CTCAACAAGTACCTGCTGGACAGCCCCTC----------------------TTCGTCACTTTCTACCAATGCCT  -22
9A  CTCAACAAGTACCTGCTGGACAGCCCCTCCCTGCAG-----TACCCCTATCTTCGTCACTTTCTACCAATGCCT  -5
9B  CTCAACAAGTACCTGCTGGACAGCCCCTC----------------------TTCGTCACTTTCTACCAATGCCT  -22
```

Mutations introduced by CRISPR-1:

```
WT  CAAGCCGTTTCTGCTGCGGGCGCTGCAGATCGCGCTGGTCGTCTCTCTCTAC
1A  CAAGCCGTTTCTGCTGCGGGCGCTGCAGATC--GCTGGTCGTCTCTCTCTAC                        -2
1B  CAAGCCGTTTCTGCTGCGGGCGCTGCAGATCG--------GTCTCTCTCTAC                        -8
2A  CAAGCCGTTTCTGCTGCGGGCGCTGCAGATCGTCTCTGCTGCGCTGGTCGTCTCTCTCTAC               +9
2B  CAAGCCGTTTCTGCTGCGGGCGCTGCAGATCG--CTGGTCGTCTCTCTCTAC                        -2
3A  CAAGCCGTTTCTGCTGCGGGCGCTGCAGATCGCCGCTGGTCGTCTCTCTCTAC                       +1
3B  CAAGCCGTTTCTGCTGCGGGCGCTGCAGATCG-----GTCGTCTCTCTCTAC                        -5
4A  CAAGCCGTTTCTGCTGCGGGCGCTGCAGATCG----GGTCGTCTCTCTCTAC                        -4

4B  CAAGCCGTTTCTGCTGCGGGCGCTGCAGATC--GCTGGTCGTCTCTCTCTAC                        -2
5A  CAAGCCGTTTCTGCTGCGGGCGCTGCAGATCGCCGCTGGTCGTCTCTCTCTAC                       +1
5B  CAAGCCGTTTCTGCTGCGGGCGCTGCAGATCGGCGCTGGTCGTCTCTCTCTAC                       +1
6A  CAAGCCGTTTCTGCTGCGGGCGCTGCAGATCGGCGCTGGTCGTCTCTCTCTAC                       +1
6B  CAAGCCGTTTCTGCTGCGGGCGCTGC-------GCTGGTCGTCTCTCTCTAC                        -7
7   CAAGCCGTTTCTGCTGCGGGCGCTGCAGATCGTCGCTGGTCGTCTCTCTCTAC                       +1
8A  CAAGCCGTTTCTGCTGCGGGCGCTGCAGATCGGCGCTGGTCGTCTCTCTCTAC                       +1
8B  CAAGCCGTTTCTGCTGCGGGCGCTGCAGATCGCGCGCTGGTCGTCTCTCTCTAC                      +2
8C  CAAGCCGTTTCTGCTGCGGGCGCTGCAGATCGACGCTGGTCGTCTCTCTCTAC                       +1
```

Accepted Article

Figure legends

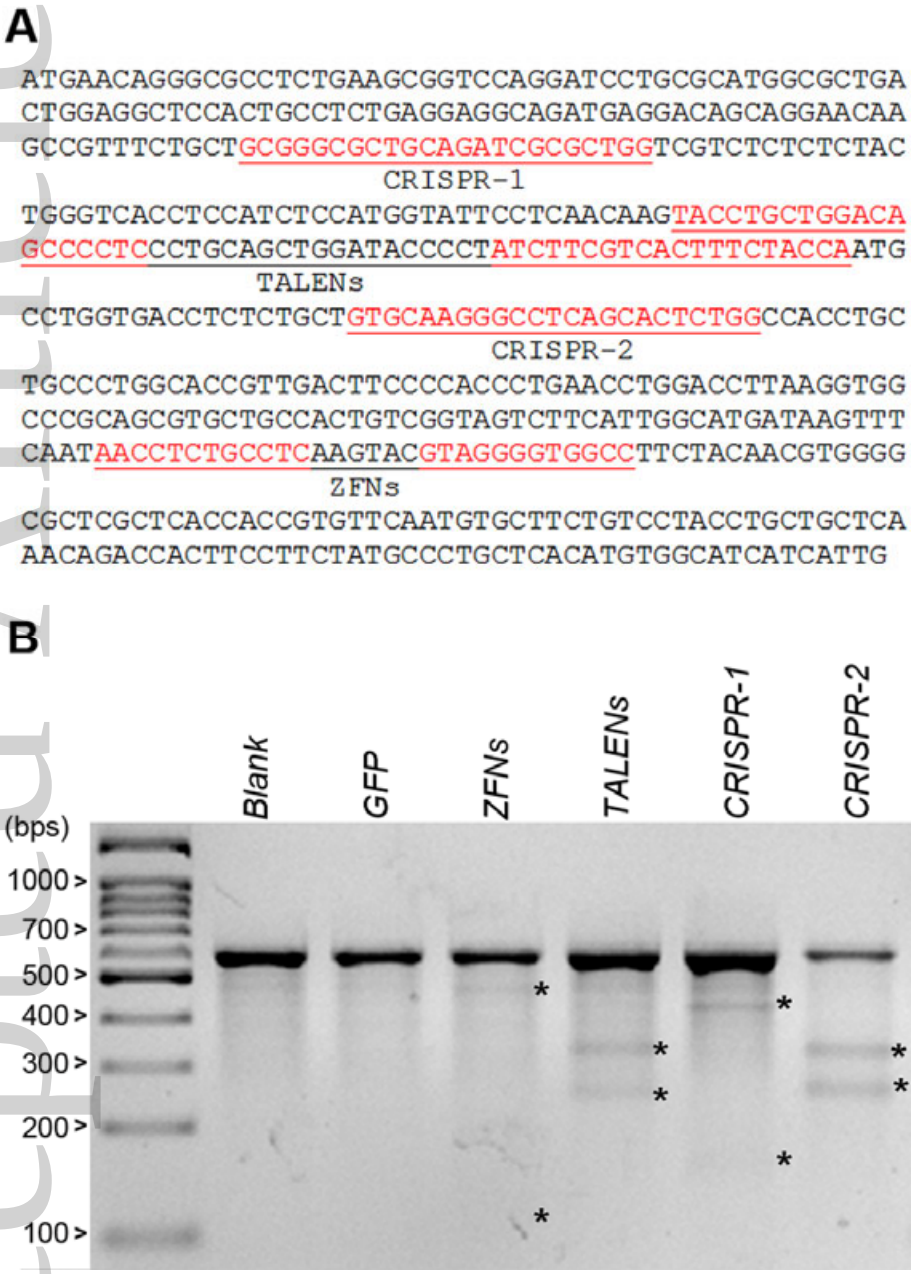

Fig. 1. Design of ZFNs, TALENs and CRISPRs to target the *Slc35c1*gene in CHO cells. (A) The binding site sequences for the ZFNs, TALENs and CRISPRs are highlighted in red (underlined). The open reading frame of GDP-fucose transporter in CHO cells is encoded by two exons and the sequence shown here is the first exon of the coding region. The two binding sites for the ZFNs are separated by 6 bps. The two binding sites for the TALENs are separated by 19 bps. Two sites were chosen for CRISPR-Cas9 targeting, namely CRISPR-1 and CRISPR-2. (B) T7E1 mismatch assay to assess the gene modification activities of the designed ZFNs, TALENs and CRISPRs. Genomic DNA of transfected cells was extracted

Accepted Article

and used as a template for PCR amplification of the region containing the target sites. Purified PCR products were heated and reannealed slowly. They were then digested with the mismatch-sensitive T7 endonuclease 1 (T7E1) that specifically recognizes and cleaves heteroduplexes formed by the hybridization of wild-type and mutant DNA sequences. Asterisks indicate the positions of the T7E1 digestion products.

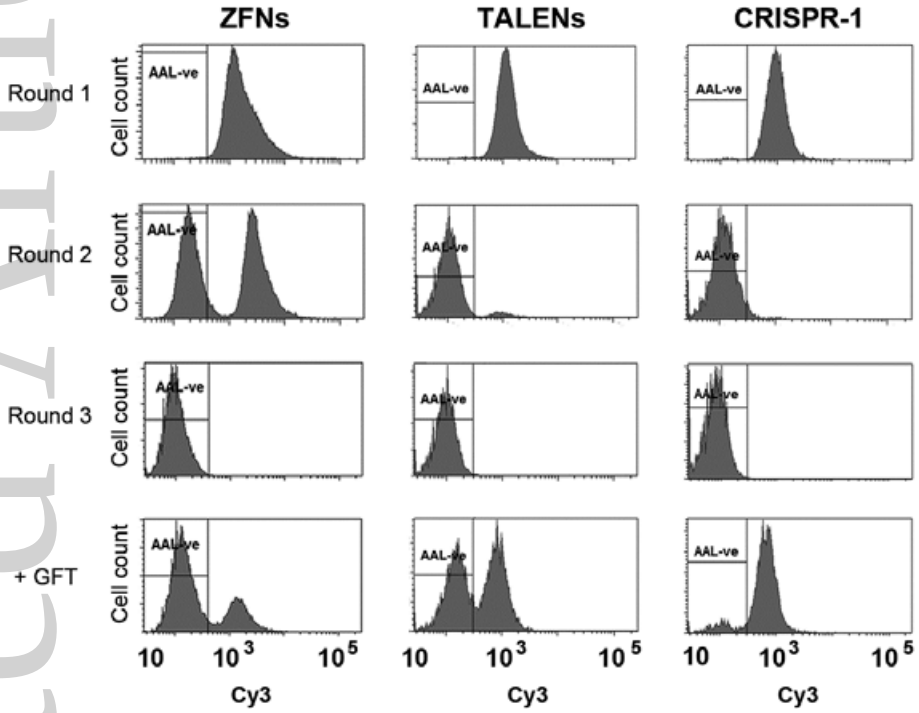

Fig. 2. FACS approach to enrich and isolate GDP-fucose transporter mutant cells generated by ZFNs, TALENs and CRISPRs. CHO-K1 cells were transfected with plasmids encoding the ZFNs, TALENs or CRISPRs. Transfected cells were labelled with biotinylated AAL and Cy3-conjugated streptavidin and the negatively stained cells were isolated by FACS. First round of FACS showed that most of transfected cells were AAL-positive (AAL+ve). The sorting gate for AAL-negative (AAL-ve) cells was set based on unstained CHO cells and the lowest 0.5% of AAL-stained cells were collected and cultured for next round of FACS. Homogeneous population of AAL-ve cells was obtained from each transfected pool after two rounds of FACS. Transfection with human GDP-fucose transporter cDNA rescues the AAL-staining phenotype (+ GFT), confirming that these AAL-ve cells lack functional GDP-fucose transporter.

Accepted Article

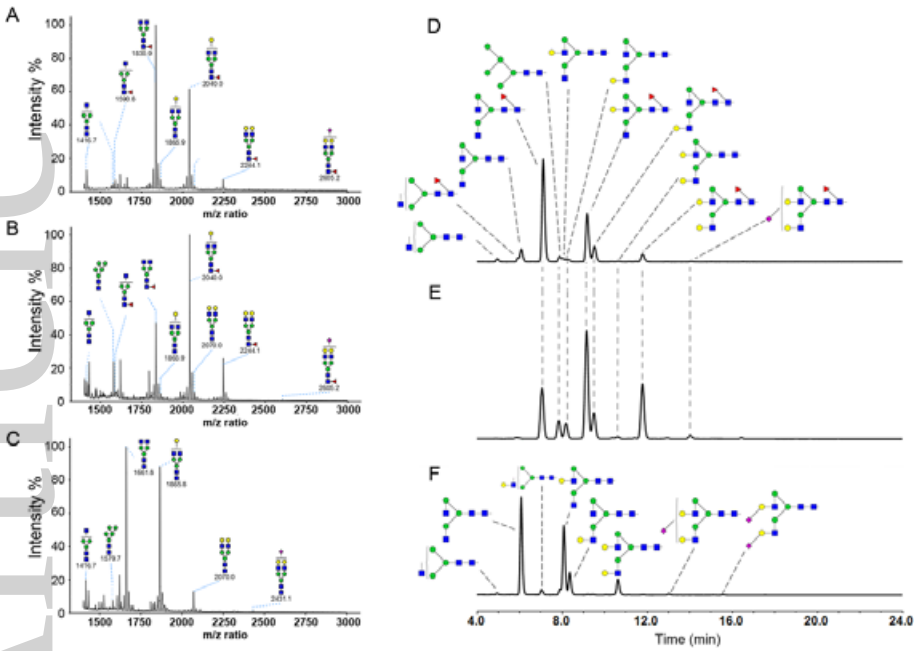

Fig. 3. MALDI-TOF and HILIC-UPLC profiling of *N*-glycans on trastuzumab (Herceptin®) and recombinant anti-Her2 antibodies produced by the parental and mutant CHO cells. *N*-glycans in each antibody preparation were analyzed by MALDI-TOF (A – C) and HILIC-UPLC-QTOF (D – F). For MALDI-TOF experiments, putative glycan structures were assigned by composition matching with theoretical masses of biochemically possible *N*-glycan structures in CHO cells. For HILIC-UPLC-QTOF experiments, glycan structure assignment was done by library search of GU values, exoglycosidase array fingerprinting, and accurate mass. Only major structures were shown here. Majority of the *N*-glycans on Herceptin (produced by Roche) (A and D) and our anti-Her2 antibody produced by the parental line (B and E) are fucosylated species such as FA2 (or G0F), FA2G1 isomers (or G1F) and FA2G2 (or G2F). In contrast, no fucosylated *N*-glycan was detected from mutant-produced anti-Her2 antibody (C and F). Note the consistent glycan profiles under both MALDI-TOF and HILIC-UPLC conditions.

Accepted Article

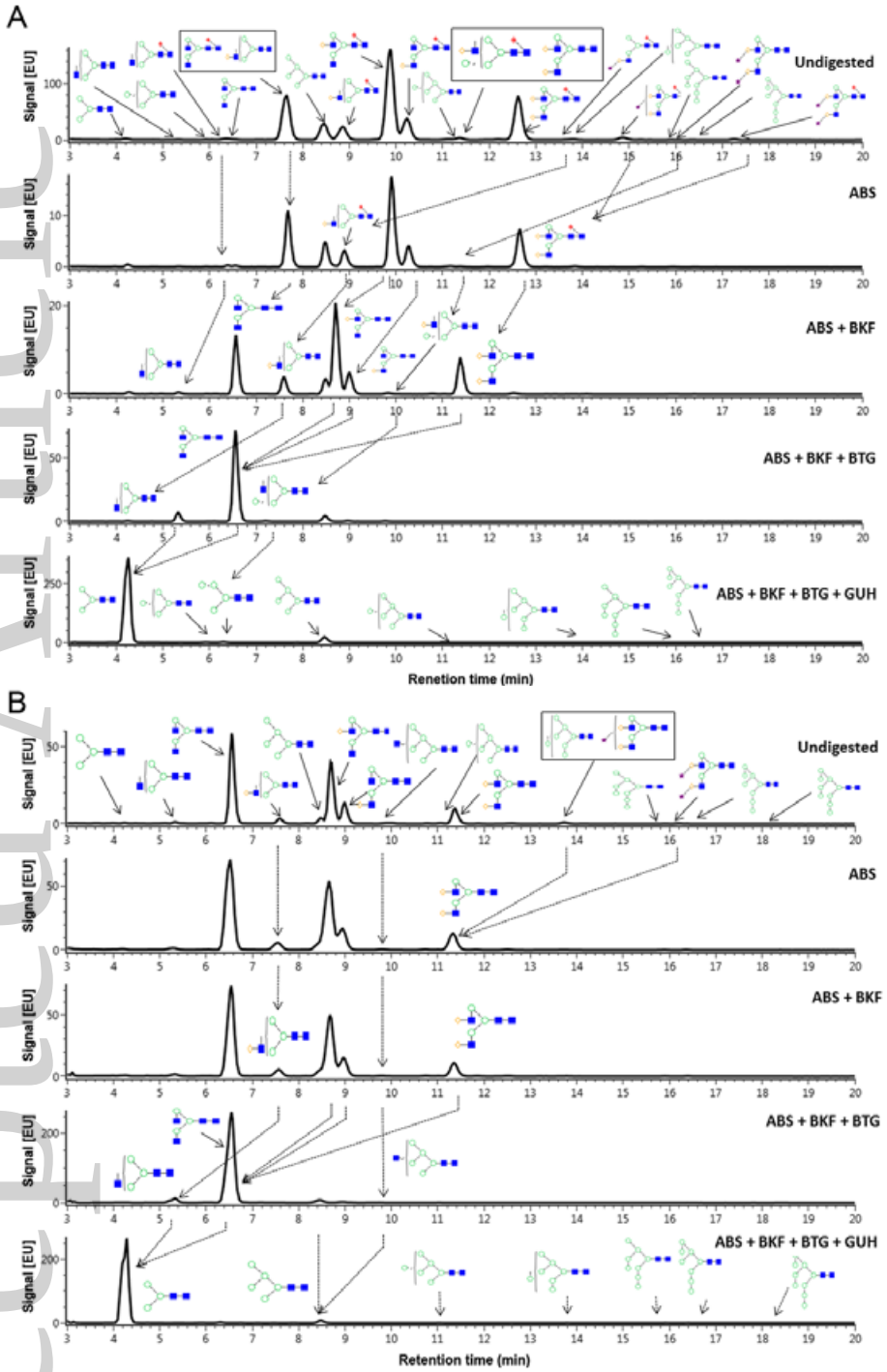

Fig. 4. Structure elucidation of *N*-glycans on parental- and mutant-produced anti-Her2 antibody by exoglycosidase digestions. 2-AB-labeled *N*-glycans were analyzed by HILIC-UPLC-QTOF with or without prior incubation with different exoglycosidases as indicated. Linkage-specific glycan structures were ascertained by following the movement of the corresponding chromatographic peaks as a result of the enzymatic removal of terminal monosaccharides. (A) Such enzymatic fingerprinting analysis revealed the presence of several truncated glycans (M4, A2G1, FM4A1G1) that are closely associated with other more commonly observed structure on HILIC-UPLC. (B) Exoglycosidase array finger printing

Accepted Article

analysis further confirmed the total absence of fucosylated *N*-glycans on mutant-produced anti-Her2 antibody. Exoglycosidases used in this experiment are: Arthrobacter ureafaciens sialidase (ABS), bovine kidney α-fucosidase (BKF), bovine testes β-galactosidase (BTG) and Streptococcus pneumoniae β-N-Acetylhexosaminidase (GUH).

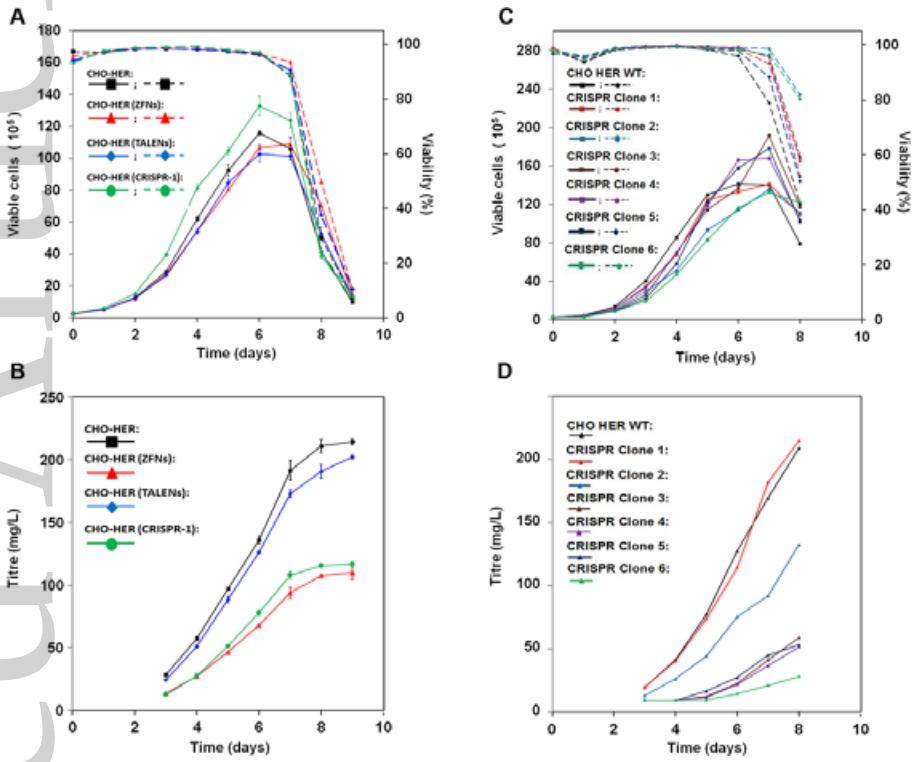

Fig. 5. Growth and productivity analysis of GDP-fucose transporter mutants generated by the ZFNs, TALENs and CRISPR-1. (A) Viable cell density and viability of the mutant pools, CHO-HER (ZFNs), CHO-HER (TALENs) and CHO-HER (CRISPR), were compared with parental anti-Her2 antibody-producing CHO-HER cells. Standard deviation (sd) was obtained from the cell count number for triplicate samples. Growth curve was plotted using mean ± sd. Dotted lines: Viability. Solid lines: Viable cells/ml. (B) Antibody production by mutant CHO-HER (ZFNs), CHO-HER (TALENs), CHO-HER (CRISPR) and parental CHO-HER were measured using the nephelometric method from day 3 to day 9. (C) Viable cell density and viability of the parental CHO-HER cells and the 6 single clones isolated from the CRISPR-1-generated mutant pool (CRISPR Clone 1 to CRISPR Clone 6). (D) Titers of the antibody produced by the parental CHO-HER cells and the 6 single clones isolated from the CRISPR-generated mutant pool.

Accepted Article